

Online Electrochemical Reduction of Both Inter- and Intramolecular Disulfide Bridges in Immunoglobulins

Martijn M. Vanduijn,* Hendrik-Jan Brouwer, Pablo Sanz de la Torre, Jean-Pierre Chervet, and Theo M. Luider



Cite This: *Anal. Chem.* 2022, 94, 3120–3125



Read Online

ACCESS |



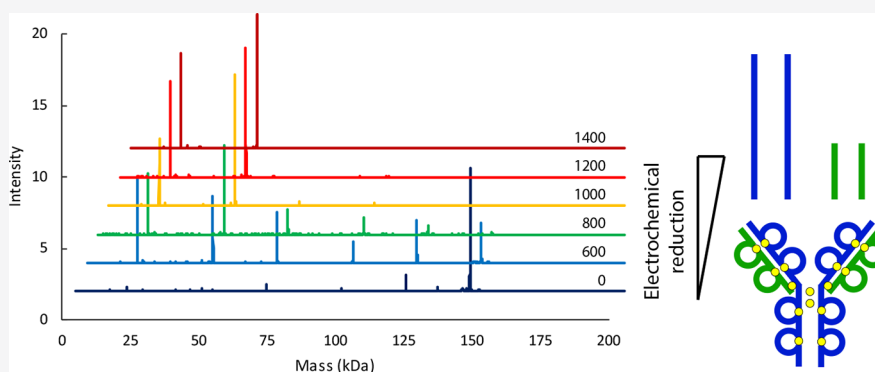
Metrics & More



Article Recommendations



Supporting Information



ABSTRACT: Electrochemical reduction of intermolecular disulfide bridges has previously been demonstrated in immunoglobulins but failed to achieve reduction of intramolecular bonds. We now report an improved method that achieves the full reduction of both intermolecular and intramolecular disulfide bridges in a set of monoclonal antibodies based on their intact mass and on MS/MS analysis. The system uses an online electrochemical flow cell positioned online between a chromatography system and a mass spectrometer to give direct information on pairs of heavy and light chains in an antibody. The complete reduction of the intramolecular disulfide bridges is important, as the redox state affects the intact mass of the antibody chain. Disulfide bonds also hamper MS/MS fragmentation of protein chains and thus limit the confirmation of the amino acid sequence of the protein of interest. The improved electrochemical system and associated protocols can simplify sample processing prior to analysis, as chemical reduction is not required. Also, it opens up new possibilities in the top-down mass spectrometry analysis of samples containing complex biomolecules with inter- and intramolecular disulfide bridges.

Many proteins use disulfide bridges between cysteine residues to stabilize their folded structure and in order to covalently associate in multi subunit complexes. For the study of such proteins, it can be advantageous to perform chromatography separations, while such disulfide links are still intact. Yet, the disulfide links can complicate downstream analysis methods, for example, mass spectrometry analysis. It is possible to collect chromatographic fractions of a sample and to subject such fractions to chemical modification, such as a reduction or proteolytic digestion. However, such methods may be time-consuming, they can be affected by undesired side reactions, and low abundance sample components are easily lost by adsorption to the collection surfaces or during sample cleanup steps that may be required before analysis is continued.

An alternative method for the reduction of disulfide bonds is by means of electrochemistry (EC) using a flow cell equipped with metal electrodes. When appropriate potentials are applied to the electrodes, disulfide bridges within sample molecules can be reduced inside the flow cell. An online coupling of the

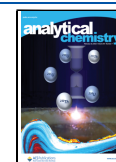
effluent of the flow cell to the electrospray ionization source of a mass spectrometer is readily achieved for analysis of protein mass and, upon activation and fragmentation in the instrument, sequence analysis is possible based on MS/MS spectra.

Electrochemical oxidation and reduction of molecules including protein disulfide bridges have been possible for some time, also with commercially available devices.^{1–6} However, new insights continually drive improvements into the design and composition of electrode materials, flow cell geometry, and the potentials applied to the active surfaces. In previous reports on immunoglobulin substrates, the reduction of intermolecular disulfide bridges and the release of heavy and

Received: September 30, 2021

Accepted: January 18, 2022

Published: February 4, 2022



light chains of the molecule were achieved, but not the reduction of the intramolecular disulfide bridges.⁷ Similarly, partial reduction of intramolecular disulfides has been observed in a hydrogen deuterium exchange setup, but complete reduction could not be achieved.⁸ The reduction of such intramolecular bridges is important for mass spectrometry analysis. First, the measured mass of the protein chain is affected, yielding 2 Da less for every disulfide pair that remains closed, which needs to be accounted for. More importantly, the closed disulfide bridges can interfere with fragmentation during MS/MS, or yield fragments that are difficult to predict and analyze with standard software tools. More recent work did achieve full electrochemical reduction in a setup that implemented reduction before chromatographic separation.⁹ We now report that the complete online reduction of both intermolecular and intramolecular disulfide bridges could be implemented after chromatographic separation, resulting in co-elution of reduced chains that had been connected by disulfide bonds in the sample. This enables experiments that study the pairing of protein chains, especially for more complex samples that require chromatographic separation prior to mass spectrometry analysis.

MATERIALS AND METHODS

Electrochemistry. Reductions were performed in a μ PrepCell-SS flow cell controlled by a ROXY Exceed potentiostat using Dialogue Elite software (Antec Scientific, Zoeterwoude, The Netherlands). The μ PrepCell is a dual electrode flow cell consisting of a titanium inlet block acting as the working electrode and a replaceable platinum counter electrode (CE). The cell volume is defined by a silicone O-ring seal and a stainless-steel spacer (150 μ m), which generates a volume of approximately 19 μ L. The flow rate through the cell was fixed at 20.0 μ L/min.

Reductions were performed in pulse mode, using a two-step potential waveform alternating between the specified potential (E_1) for 1 s and 0.0 mV (E_2) for 0.1 s configured with the instrument software. E_1 is the potential driving disulfide bridge reduction, whereas E_2 represents a short cleaning step.

Chromatography. Separations were performed on a Waters BEH C4 column (100 mm \times 150 μ m, 1.8 μ m particles, 300 Å pore) on a Dionex Ultimate 3000 chromatography system. The protein sample (500 ng on the column) was trapped and desalted on a trap column (Thermo Scientific PepMap 300 Å C4 0.3 mm \times 5 mm) with 0.1% formic acid as a loading solvent before a gradient separation over the analytical column. The analytical gradient consisted of 0.1% formic acid (A) and 0.08% formic acid and 80% acetonitrile in water (B), running from 4 to 90% (B) in 25 min at a flowrate of 1 μ L/min and 40 °C. Post-column, 19 μ L/min 1% formic acid, 50% acetonitrile in water was introduced in a Waters nano-Tee as a makeup flow in order to increase the flowrate through the electrochemical cell to a total of 20 μ L/min to elevate the concentration of formic acid for effective reduction and also to elevate the concentration of acetonitrile for a stable electrospray (Figure 1).

Mass Spectrometry. Mass spectra were recorded on an Orbitrap Fusion Lumos (Thermo Fisher Scientific, Bremen, Germany) equipped with the H-ESI atmospheric pressure interface, scanning at a resolution of both 120,000 and 15,000 for MS1 spectra and 60,000 for (targeted) MS2 spectra. Also, where indicated, spectra were recorded on a Waters Synapt G2-Si Q-TOF in resolution mode. Nonisotopically resolved

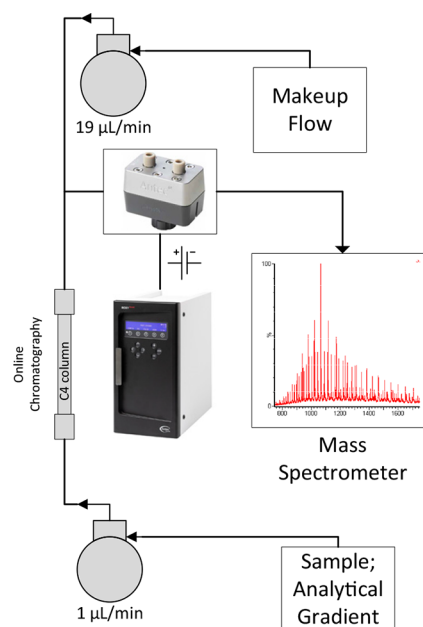


Figure 1. Fluidics diagram. Implementation of the makeup flow and the online coupling of chromatography, electrochemical cell, and mass spectrometer.

spectra were deconvoluted using the UniDEC deconvolution tool¹⁰ high-resolution Orbitrap spectra with the vendor Xtract algorithm in the Freestyle 1.6 application (Thermo Fisher Scientific). Top-down MS/MS spectra were matched using ProSight Lite 1.4.¹¹ The mass spectrometry proteomics data have been deposited to the ProteomeXchange Consortium via the PRIDE partner repository with the data set identifier PXD021649.¹²

Antibody Molecules. The study was performed on the monoclonal antibodies (mAb): bevacizumab (Roche), panitumumab (Amgen), pembrolizumab (Merck), cetuximab (Eli Lilly and Co), adalimumab (Abbott), and alemtuzumab (Genzyme). bevacizumab Fab fragment was prepared with Fabalactica protease (Genovis). For chemical reduction controls, a denatured solution was prepared of 2.5 mg/mL bevacizumab in 6 M guanidine HCl, 25 mM Tris pH 7.4, and 10 mM DTT. The reduction was allowed to take place for 30 min at 60 °C before diluting the sample 1:10 in 0.1% aqueous formic acid. As a negative control, bevacizumab was incubated the same except for the presence of DTT. A third sample was bevacizumab incubated with 10 mM DTT under native conditions (25 mM Tris pH 7.4, 37 °C, 30 min). Under these conditions, heavy and light chains are separated by reduction of disulfides, but most intramolecular disulfides were found to remain intact, presumably due to the protein folding preventing access for the DTT in the solution. Upon dilution into formic acid, proteins may denature due to low pH. However, the reducing activity of DTT at low pH is negligible.

RESULTS

Reduction of Intermolecular Disulfide Bonds of IgG. Immunoglobulins consist of a distinct heavy chain and a light chain bonded by a single disulfide bridge. In addition, disulfide bridges exist between the heavy chains of two such heterodimers, yielding a covalently bonded complex of two heavy chains and two light chains. Upon full reduction, the heavy chain (50 kDa) and light chain (25 kDa) molecules are

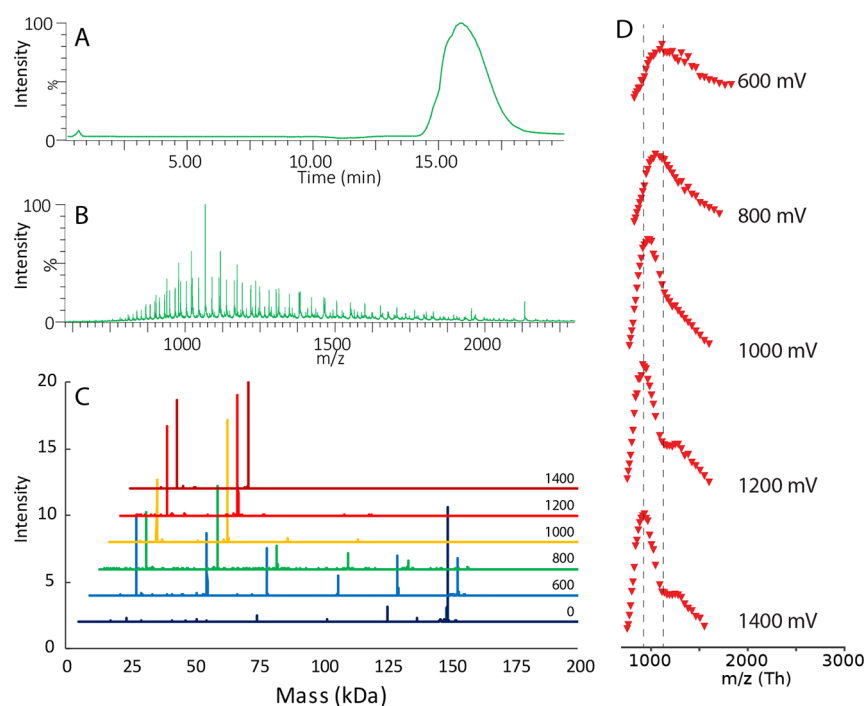


Figure 2. Electrochemical reduction of bevacizumab to separate heavy and light chains. (A) Representative chromatographic profile (total ion current, 800 mV potential). (B) Q-TOF mass spectrum averaged across the chromatographic peak (800 mV; other potentials shown in Figure S1). (C) Waterfall plot of deconvoluted mass spectra for different electrochemical potentials (mV potential annotated). (D) Peak apex from MS1 spectra, associated with the heavy chain by deconvolution analysis. Dotted lines highlight the shift in charge state distribution from 600 to 1400 mV. One charge state apex was omitted due to overlap with the light chain envelope. Full annotated spectra are given in Figure S2.

liberated from this complex, but partial reduction may yield complexes of an intermediate stoichiometry as well.

We use a setup that implements an online coupling of mass spectrometry and EC. This enables useful applications of the reduction method, but also is more challenging due to the limited concentration and residence time of the analytes in the cell.

In top-down proteomics—the mass spectrometry analysis of intact protein molecules—smaller protein chains tend to be more easily detected and analyzed. Thus, a more detailed analysis could be performed based on data for the light chain of the IgG molecule. The electrochemical reduction of intact IgG to the light and heavy chain components was assessed on a time of flight mass spectrometer, as this gave a better signal for the intact IgG and heavy chains. As shown in Figure 2A, all samples were eluted from a chromatography system for online reduction and mass spectrometry. As indicated in panels B and C, heavy and light chains could be liberated from the intact bevacizumab sample and were co-eluted. The reduction potential of the electrochemical cell was varied in order to assess the optimal settings for separation of the chains. Complete reduction was found at 1000 mV, and partial reduction was found at lower potentials. Also, it was found that increases in the potential beyond the requirements for disulfide reduction adversely affected noise in the mass spectra that were recorded (not shown). The generation of gasses from the electrochemical hydrolysis of water at such potentials may affect the stability of the electrospray as well as the accessible area of the electrode surface. Heavy and light chain charge envelopes could be seen as soon as reduction of the intermolecular bond started. However, with increasing electrochemical potentials, an additional shift in the distribution of the charge states could be observed for both the light and

heavy chains, favoring more highly charged species at higher reduction potentials (Figure 2D).

Reduction of Intramolecular Disulfide Bonds of IgG.

The signals of separated heavy and light chains from a sample of intact bevacizumab confirmed that the electrochemical system could reduce the intermolecular disulfide bridges. However, a system capable of reducing both intra- and intermolecular disulfide bridges would be more useful for practical applications. The detection of successful reduction of intramolecular bonds is more challenging, as the reduction products exhibit only a small mass shift compared to the parent compound. Two reduced cysteine residues with a free $-SH$ group contain two additional hydrogens compared to a $S-S$ bonded cysteine pair, amounting to 2.016 Da mass increase for each reduced cysteine pair. With two internal disulfide bridges in the light chain, the maximum expected mass shift is 4.032 Da. While this is easily resolved by the mass spectrometer, the isotopic envelopes of the protein signals are wider than that, resulting in overlapping spectra for mixtures of chains with 0, 1, or 2 reduced disulfide intramolecular bonds.

The degree of reduction can be assessed qualitatively by inspecting the distribution of charge states of the protein chain MS1 signals. A fully reduced chain is free to unwind, while disulfide bridges can hold the chain in a partially coiled or folded configuration. In the folded chain, fewer residues are accessible for protonation during the electrospray ionization. Hence, the distribution of charge states in a fully reduced chain is shifted toward a higher charge (lower m/z) than in the case of intact disulfide bridges. Indeed, such shifts could be observed in the MS1 data (Figures 2D and S2).

To obtain a more quantitative assessment on the contribution of each redox form to the mixed signal in the experimental data, we simulated the isotopic envelope of each

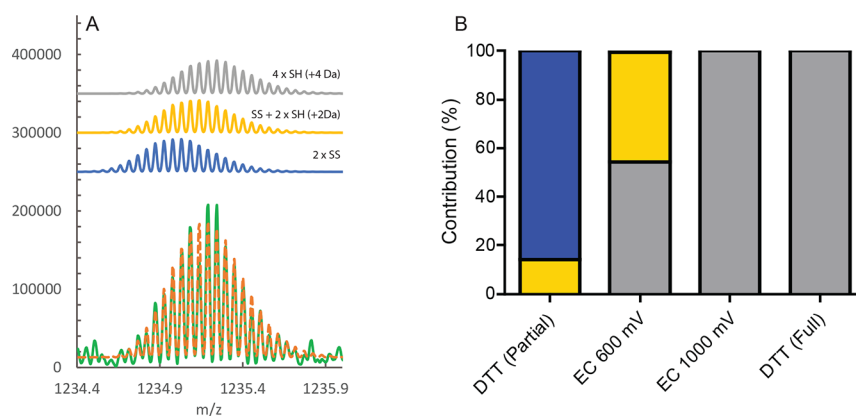


Figure 3. Assessment of intramolecular disulfide reduction from MS1 spectra. (A) Top panel: simulated spectra for the redox forms of bevacizumab light chain 19⁺ that were used to fit to the experimental data. Blue: both SS intact. Yellow: one SS reduced. Gray: both SS reduced. Bottom panel: green: experimental data; dashed brown: best fit (weighted sum of forms shown in the top panel). The analysis is for electrochemical reduction with a 600 mV potential; other conditions are given in Figure S3. (B) Relative contributions of each redox form in the best fit to the experimental data after chemical and electrochemical reductions (EC). Colors as in panel A. Partial reduction was with DTT under native conditions, and full reduction was under denaturing conditions.

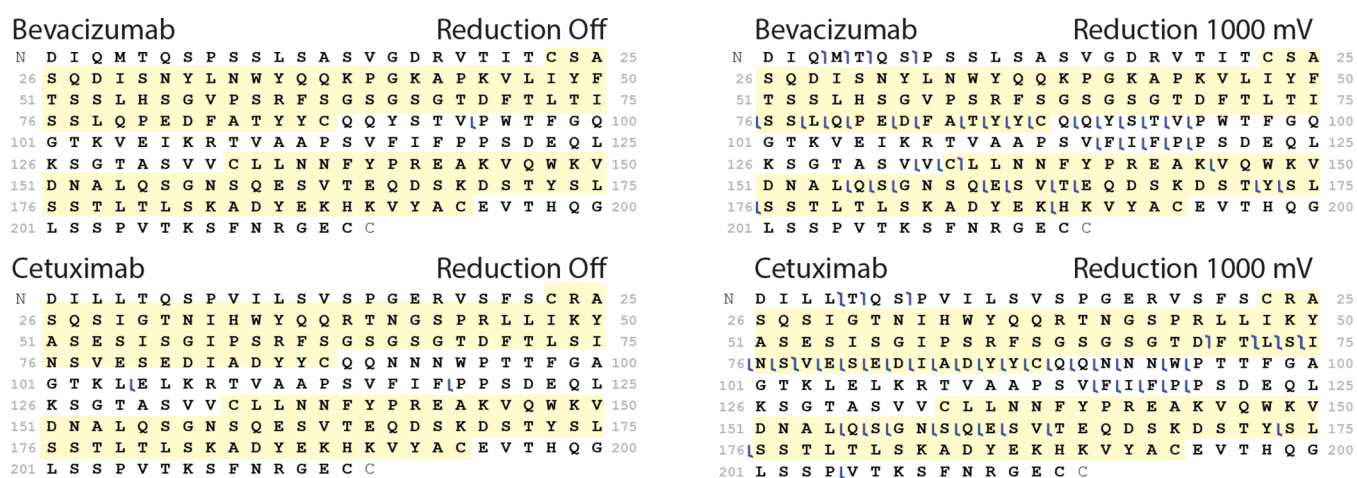


Figure 4. Assessment of intramolecular disulfide reduction from MS/MS spectra. With electrochemical reduction disabled or at 1000 mV, data were recorded from 19⁺ light chain precursors of bevacizumab or cetuximab fragmented by HCD (normalized collision energy 34). The resulting spectra were deconvoluted and matched to the sequence of the chains. Matching b and y ions (100 ppm) were highlighted in the sequence, and yellow boxes show the region between cysteines that form a disulfide bridge in the native mAb. Data from additional mAbs are shown in Figure S5; mass errors are plotted in Figure S6.

19⁺ redox form of bevacizumab light chain (Xcalibur Qualbrowser, Thermo Fisher Scientific). To model spectra of a mixture, a sum of these redox forms was calculated in tabular data, with a coefficient applied for the three contributing spectra as $\text{sum} = a \cdot \text{reduced} + b \cdot \text{semi-reduced} + c \cdot \text{oxidized}$. The coefficient a , b , and c for each redox form in this sum was fitted to minimize the sum of squares difference of the modeled spectrum with the experimental data (Excel solver). The fitted spectrum in all cases approximated the experimental data and indicated that the electrochemical reduction was capable of producing the fully reduced form of the bevacizumab light chain molecule without detectable amounts of forms with intact intramolecular disulfide bridges (Figure 3). At lower potentials in the electrochemical cell, a mix of redox states was observed, indicating that the disulfide bridges were not reduced completely and that some chains had only one intramolecular disulfide bridge reduced rather than both. Based on the mass, it is not possible to distinguish whether there is a bias for which of the intramolecular disulfide bridges is reduced first and which one remains intact. Also, this analysis does not

provide information on other isoforms resulting from hydrogen transfer or from shuffling of disulfide bonds that differ by only 1 Da.

The reduction of mAbs other than bevacizumab was evaluated as well. The masses of their light chains after electrochemical reduction are reported in Table S1 and are also consistent with a complete reduction of the light chain under these conditions. Data were also obtained on reduction of the heavy chain, although their signals were not well resolved for all mAbs (Table S2 and Figure S4). The deconvoluted masses were compared to the predicted mass of the heavy chains after accounting for loss of the C-terminal lysine and the formation of pyroglutamic acid on the N-terminus and glycosylation with G0F or G1F glycans. The available data are consistent with a full reduction of the heavy chain as well as the light chain.

MS/MS Fragmentation Analysis of Electrochemically Reduced IgG. One possible benefit of the electrochemical reduction of intramolecular bonds is the acquisition of better MS/MS data. In particular, incomplete reduction could affect

the fragmentation of stretches of protein between disulfide bonded cysteine residues. MS/MS data were assessed for a set of seven mAbs, two of which are shown in Figure 4 and the remaining ones are shown in Figure S5. The 19^+ reduced light chain of each mAb was isolated and fragmented with higher energy collisional dissociation (HCD). After deconvolution, the fragments were matched to the sequence of the light chains. A tolerance of 100 ppm was applied, as deconvolution may be prone to misassignment of the monoisotopic mass by 1 Da. Still, most fragments matched the predicted mass by less than 10 ppm (Figure S6). A correct mass assignment also indicates that disulfide bridges that are located N-terminal to the b-ion break or c-terminal to the y-ion break are in the reduced state, as a closed disulfide bridge would subtract 2 Da from the mass. This could be observed in MS/MS data on bevacizumab that were reduced by DTT under native conditions which leave the intramolecular disulfide bridges intact. In these data, many more matches are found after accounting for the change in mass due to closed disulfide bridges (Figure S7). Moreover, very few fragments are observed from residues between bridged disulfides, suggesting that the fragmentation is impaired in this partially reduced state, but not in the fully reduced state.

MS/MS analysis was also performed on a bevacizumab heavy chain from a Fab fragment, as such truncated heavy chains yield data that are more readily interpreted. Again, a series of fragments was observed from a region enclosed by a potential disulfide bridge, confirming that the intramolecular disulfide bridges had been electrochemically reduced (Figure S8).

DISCUSSION

Electrochemical redox reactions can be useful modalities in small molecule research (metabolism models), and increasingly also in protein research. Prior studies already demonstrated that electrochemical methods can successfully be applied for the reduction of many disulfide bridges that connect protein chains, or for complex cysteine topologies such as cysteine knots. However, a complete reduction of the sample is important in order to achieve the analytical goals. Such analytical goals may include determining the accurate mass of a protein, obtaining sequence information of a protein, or obtaining information on the protein structure through hydrogen deuterium exchange type experiments. Such complete reduction was not possible for antibody molecules in online electrochemical reduction experiments until recently.

In the current work, we demonstrated that a selection of monoclonal antibodies could be fully reduced by electrochemical reduction after chromatography of the intact molecule. Both heavy and light chains were liberated until no signal could be observed from the intact mAb. The intact masses observed in deconvoluted MS spectra were consistent with reduction of both inter- and intramolecular disulfide bridges. Furthermore, the analysis of MS/MS spectra of the light chains corroborated the reduction of the disulfide bonds in the electrochemical cell, and for heavy chains, such MS/MS data were obtained from a Fab fragment.

The MS signal of the heavy chains that were obtained under these conditions was weaker and less resolved than that for the light chain, which may relate to the larger mass of the heavy chain or the splitting of the signal due to the different glycoforms of the heavy chain. This may explain why we could not resolve heavy chains for all mAb that were assessed. Where

the heavy chains could be resolved, masses were mostly consistent with full reduction. Typical IgG heavy chains contain four intramolecular disulfide bonds, and incomplete reduction forms would yield masses of 2–8 Da less than the calculated fully reduced mass. Only the G1F glycoform of denosumab showed a mass 6 Da less than expected, but the G0F glycoform of the same sample did indicate full reduction, based on a stronger signal than the G1F peak. Thus, the preponderance of evidence is that a full reduction could be achieved in our experiments for both heavy and light chains. There was no evidence for major differences between the mAbs that were tested in terms of the reduction that was achieved. While heavy chains were not always well resolved, light chains were detected well also in these samples, suggesting that reduction was similar for these mAbs and that the lack of heavy chain signal rather relates to, for example, ionization, detection, or a diversity of proteoforms.

It is of interest why the reduction of intramolecular disulfide bonds has now been successful where it has failed in the past. The first distinction is in the surface material of the flow cell that was used. The reduction occurs at a titanium surface, but the CE was platinum-plated, in contrast with older all-titanium designs. This results in a more robust surface chemistry and removes the need for regular polishing for regeneration of the CE. In previous designs, a three-electrode configuration was employed (for reference, working, and auxiliary electrodes), whereas the current design has been reduced to two electrodes. The potential profile driving the reduction was adapted to this revised electrode configuration. Finally, it is possible that the conditions of the make-up liquid (50% acetonitrile and 1% formic acid) are more favorable for reduction, for example, by stronger denaturation of the protein chains. In the recent work by Morgan et al., a full reduction could be obtained only after the application of heat during reduction.⁹ Their findings fit with the hypothesis that denaturing conditions are important for achieving full electrochemical reduction and mirror protocols for full chemical reduction of immunoglobulins that typically require denaturation with, for example, urea or guanidine hydrochloride.

The only aspect of the potential profile that was varied during our current experiments was the amplitude. In general, we found that potentials below 500 mV did not result in disulfide reduction, potentials around 1000 mV were optimal for this application, and potentials in excess of the optimum adversely affected results, mostly through a poor signal to noise ratio in the recorded mass spectra that possibly results from the introduction of gas bubbles from the electrolysis of water in the cell. It was also observed that the onset of reduction did not always occur at the same potential during our experiments. Hence, the use of a potential 100 mV over the apparent optimum would probably benefit robust operation.

Other parameters that may affect the reduction yields are the flow rate through the cell and the amount and concentration of the analyte that is passed through the cell. In all experiments, 500 ng was loaded on the column, which was chosen as the minimum amount to give robust results. While it was clear that more samples could be reduced per injection, we did not explore the limit, as this might also result in excessive deposits in the ion source of the mass spectrometer. In terms of flow rate, the chosen condition (20 $\mu\text{L}/\text{min}$) was a compromise between sample dispersion and dilution. In our setup, the analytical column utilizes a lower flow rate than the electrochemical cell. An advantage of this setup is the

opportunity to have more control over solvent conditions in the electrochemical cell. In our work, these were almost constant at 1% formic acid and 50% acetonitrile. The formic acid content is higher than the 0.1% commonly used in reversed phase chromatography, but is important to promote the reduction, possibly as a reaction partner.^{13,14}

The post-column reduction setup with makeup flow allows for conventional conditions during separation but full control on the reduction environment. Furthermore, this post-column configuration will result in co-elution of reduced chains that were still connected by a disulfide bridge during chromatography. While this is not beneficial when performing an analysis on a single purified mAb, the design allows for separation of more complex samples prior to reduction. In this way, the pairing between protein chains in the mixture could be revealed.

CONCLUSIONS

We are encouraged that electrochemical reduction could be positioned online between LC and MS stages of the experiment and it yielded sufficient data by both MS and MS/MS during the chromatographic peak for comparison with a reference database. Future improvements could focus on a decrease of the flow cell volume in the electrochemical system. While the currently chosen implementation with a makeup flow has certain benefits, it is expected that sensitivity and chromatographic parameters could benefit from an adaptation of flow cell volume and overall flow rate. Regardless, the current work demonstrates that it is already feasible to completely reduce the inter- and intramolecular disulfide bridges in immunoglobulins with an electrochemical system that is coupled online between a chromatography system and a mass spectrometer.

ASSOCIATED CONTENT

Supporting Information

The Supporting Information is available free of charge at <https://pubs.acs.org/doi/10.1021/acs.analchem.1c04261>.

Monoisotopic masses, experimental and modeled MS1 spectra, MS/MS fragment analysis and mass errors (PDF)

AUTHOR INFORMATION

Corresponding Author

Martijn M. Vanduijn – Department of Neurology, Erasmus MC, 3000 CA Rotterdam, The Netherlands; orcid.org/0000-0002-6654-994X; Email: m.m.vanduijn@erasmusmc.nl

Authors

Hendrik-Jan Brouwer – Antec Scientific, 2382 NV Zoeterwoude, The Netherlands; orcid.org/0000-0002-5194-1463

Pablo Sanz de la Torre – Antec Scientific, 2382 NV Zoeterwoude, The Netherlands

Jean-Pierre Chervet – Antec Scientific, 2382 NV Zoeterwoude, The Netherlands

Theo M. Luider – Department of Neurology, Erasmus MC, 3000 CA Rotterdam, The Netherlands; orcid.org/0000-0003-1962-561X

Complete contact information is available at: <https://pubs.acs.org/10.1021/acs.analchem.1c04261>

Author Contributions

The manuscript was written through contributions of all authors. All authors have given approval to the final version of the manuscript.

Notes

The authors declare the following competing financial interest(s): The authors declare the following: HJB, PST and JPC are employed at Antec Scientific B.V., the manufacturer of the electrochemical instrumentation used in this research. The Erasmus MC has a sponsored research agreement with Antec Scientific. There is no conflict of interest.

ACKNOWLEDGMENTS

This work was supported in part by STW grant 14325 to Erasmus MC and Antec Scientific.

REFERENCES

- (1) Zhang, Y.; Cui, W.; Zhang, H.; Dewald, H. D.; Chen, H. *Anal. Chem.* **2012**, *84*, 3838–3842.
- (2) Zhu, L.; Santiago-Schübel, B.; Xiao, H.; Hollert, H.; Kueppers, S. *Water Res.* **2016**, *102*, 52–62.
- (3) König, A.; Weidauer, C.; Seiwert, B.; Reemtsma, T.; Unger, T.; Jekel, M. *Water Res.* **2016**, *101*, 272–280.
- (4) Li, J.; Dewald, H. D.; Chen, H. *Anal. Chem.* **2009**, *81*, 9716–9722.
- (5) Zheng, Q.; Zhang, H.; Chen, H. *Int. J. Mass Spectrom.* **2013**, *353*, 84–92.
- (6) Bütter, L.; Frensemeier, L. M.; Vogel, M.; Karst, U. *J. Chromatogr. A* **2017**, *1479*, 153–160.
- (7) Nicolardi, S.; Deelder, A. M.; Palmblad, M.; van der Burgt, Y. E. M. *Anal. Chem.* **2014**, *86*, 5376–5382.
- (8) Trabjerg, E.; Jakobsen, R. U.; Mysling, S.; Christensen, S.; Jørgensen, T. J. D.; Rand, K. D. *Anal. Chem.* **2015**, *87*, 8880–8888.
- (9) Morgan, T. E.; Jakes, C.; Brouwer, H. J.; Millan-Martin, S.; Chervet, J. P.; Cook, K.; Carillo, S.; Bones, J. *Analyst* **2021**, *146*, 6547–6555.
- (10) Marty, M. T.; Baldwin, A. J.; Marklund, E. G.; Hochberg, G. K. A.; Benesch, J. L. P.; Robinson, C. V. *Anal. Chem.* **2015**, *87*, 4370–4376.
- (11) Fellers, R. T.; Greer, J. B.; Early, B. P.; Yu, X.; LeDuc, R. D.; Kelleher, N. L.; Thomas, P. M. *Proteomics* **2015**, *15*, 1235–1238.
- (12) Perez-Riverol, Y.; Csordas, A.; Bai, J.; Bernal-Llinares, M.; Hewapathirana, S.; Kundu, D. J.; Inuganti, A.; Griss, J.; Mayer, G.; Eisenacher, M.; Pérez, E.; Uszkoreit, J.; Pfeuffer, J.; Sachsenberg, T.; Yilmaz, S.; Tiwary, S.; Cox, J.; Audain, E.; Walzer, M.; Jarnuczak, A. F.; Ternent, T.; Brazma, A.; Vizcaíno, J. A. *Nucleic Acids Res.* **2019**, *47*, D442–D450.
- (13) Stocks, B. B.; Melanson, J. E. *Anal. Bioanal. Chem.* **2018**, *411*, 4729–4737.
- (14) Koch, C. J.; Raleigh, J. A. *Arch. Biochem. Biophys.* **1991**, *287*, 75–84.